A COMPREHENSIVE REVIEW OF HEAT TRANSFER IN POROUS MEDIA: FOCUSING ON NANOFLUIDS, PHASE CHANGE MATERIALS, AND NANOENCAPSULATED PHASE CHANGE MATERIALS

Hossam A. Nabwey,^{1,2,*} Behzad Azizimehr,³ Taher Armaghani,^{3,*} Ramin Ghasemiasl,³ Narjes Yaqoub Alamdar,⁴ A.M. Rashad,⁵ & Ali J. Chamkha⁶

- ¹Department of Mathematics, College of Science and Humanities in Al-Kharj, Prince Sattam Bin Abdulaziz University, Al-Kharj11942, Saudi Arabia
- ²Department of Basic Engineering Science, Faculty of Engineering, Menoufia University, Shebin El-Kom, 32511, Egypt
- ³Department of Engineering, West Tehran Branch, Islamic Azad University, Tehran, Iran
- ⁴Department of Engineering, Dezful Branch, Islamic Azad University, Dezful, Iran
- ⁵Department of Mathematics, Faculty of Science, Aswan University, Aswan, Egypt
- ⁶Faculty of Engineering, Kuwait College of Science and Technology, Doha District, 35004, Kuwait
- *Address all correspondence to: Hossam A. Nabwey, Department of Mathematics, College of Science and Humanities in Al-Kharj, Prince Sattam bin Abdulaziz University, Al-Kharj11942, Saudi Arabia; Tel.: +0569822136, E-mail: eng_hossam21@yahoo.com; or Taher Armaghani, Department of Engineering, West Tehran Branch, Islamic Azad University, Tehran, Iran; Tel.: +00989124312885, E-mail: armaghani.taher@yahoo.com

This research investigates the recent advancements in heat transfer through nanofluids in porous media. We seek to conduct a comprehensive review of the most influential papers published since 2020, aiming to contribute significantly to this field. Initially, key parameters affecting heat transfer in porous media, such as porosity, permeability, pore shape and size, and other factors are introduced. Subsequently, the primary heat transfer mechanisms, the impact of flow velocity and patterns, heat transfer rates, thermal equilibrium and nonequilibrium conditions, and techniques to enhance heat transfer, including nanomaterials and phase change materials, are explored. Following an introduction to nanomaterials and their various types, this study delves into the methodologies for their synthesis and thermal conductivity models. Additionally, phase change materials are categorized as another effective approach to enhance heat transfer, and methods for improving their thermal conductivity are explored. A comprehensive review of recent studies, presented in tabular form, reveals that the highest heat transfer coefficient and Nusselt number for nanofluids were attained at a 30° angle and with a square porosity. In forced and mixed convection scenarios, increasing porosity and the length of the heat source led to a higher Nusselt number, whereas increasing the Hartmann number resulted in a decrease. Furthermore, a comprehensive statistical analysis of heat transfer in porous media using nanofluids demonstrated that Al₂O₃water nanofluids with a 28.33% concentration, cylindrical geometry with 27.78%, and the Darcy-Brinkman model with 33% exhibited the most significant contributions.

KEY WORDS: phase change materials, thermal conductivity, heat transfer, nanomaterials, porosity, permeability

	NOMI	ENCLATURE	
$k_{_{\mathrm{B}}}$	Boltzmann constant	Abbreviat	ions
k_{bf}^{D}	conduction factor for base	CGM	common grid model
01	fluid	CVFEM	control volume finite element
$\mathbf{k}_{_{\mathrm{p}}}$	conduction factor for		method
Р	nanoparticles	FDM	fused deposition modeling
DA	Darcy number	FEM	finite element method
V	Darcy velocity	FVM	finite volume method
d_p	diameter of the phase	GFEM	generalized finite element
$\mu_{\rm e}^{\rm p}$	effective viscosity		method
μ	fluid's viscosity	GDQLIM	generalized differential
f	frag function		quadrature element method
Gr	Grashof number	HNF	holistic niche formation
На	Hartmann number	KBM	Krylov-Bogoliubov-
C_k	mass quotient of each		Mitropolsky
K	phase	MWCNT	multi-walled carbon nanotube
Nu	Nusselt number	RSM	response surface methodology
Pr	Prandtl number	SIMPLE	semi-implicit method for
Ra	Rayleigh number		pressure linked equations
Re	Reynolds number	MHD	magnetohydrodynamics

1. INTRODUCTION

Heat transfer in porous media enhanced by nanoparticles is a cutting-edge and challenging research topic in engineering. Given its wide-ranging applications and significant importance across various industries, it has attracted substantial attention. In recent years, nanoparticles have emerged as promising additives to augment the thermal performance of heat transfer fluids. Owing to their exceptionally high specific surface area and superior thermal properties, nanoparticles can dramatically enhance the thermal conductivity and heat transfer capabilities of base fluids. The incorporation of nanoparticles into base fluids results in the creation of nanofluids, which exhibit significantly improved heat transfer characteristics and demonstrate superior performance within porous media.

2. POROUS MATERIAL

A porous material is defined as a solid matrix containing interconnected voids. Depending on whether the porous medium can allow the passage of substances under external forces, it is classified as permeable or impermeable. Porous media can be either dispersed or continuous, homogeneous or heterogeneous, composite, or a combination of different structures.

Porous materials are also known as cellular solids. The word "cell" is derived from the Latin word *cella*, which means a chamber or a closed compartment. Therefore, cellular solids are assemblies of cells that are aggregated by solid edges or faces. If the solid material is enclosed only by the edges of the cell so that the cells are connected through open faces, the material is called open-celled. If the faces are solid, each cell is separate from its neighboring cells; in this case, the material is called closed-celled (Flickinger, 2013).

Porous media properties are defined by several parameters, including the following:

- Porosity: the ratio of the volume of voids to the total volume of the porous material.
- Pore type: open, closed, or partially open.

- Permeability: the fraction of the cross-sectional area occupied by pores.
- Tortuosity: the ratio of the average pore length to the thickness of the porous medium.
- Specific surface area and pore shape.
- Viscosity and inertia coefficients of the porous medium.
- Physical and mechanical properties of the porous medium.

The permeability of a medium is generally a function of the shape and orientation of its fibers, their arrangement relative to the flow, and their distribution in different directions (Kaviany, 2012).

2.1 Permeability

Permeability is a fundamental and intrinsic property of porous media. Unlike porosity, it cannot be defined solely in terms of fluid flow but is rather a characteristic of the porous medium itself. Permeability is commonly used to estimate the rate of fluid injection or flow into a porous medium. It is defined as a proportionality constant relating the volumetric flow rate of a fluid through a porous medium to the applied pressure (potential gradient) (Nazari et al., 2013).

$$k = \frac{\mu U_d}{\nabla p}.\tag{1}$$

Initial studies in this field can be traced back to Darcy's experiments. Darcy reported a linear relationship between the pressure drop across a unit length of a porous medium and the average superficial velocity. The equation $k = \mu U_d/\nabla p$ represents Darcy's law for one-dimensional, single-phase flow and defines permeability. The coefficient k in Darcy's model represents the permeability of the porous medium in terms of square meters. In this equation, μ is the fluid viscosity, U_d is the average superficial velocity, and ∇p is the pressure drop per unit length. This relationship, frequently cited in the literature, is suitable for creeping flows (Kaviany, 2012). Darcy's law is often used to find the pressure drop, especially where the flow regime is creeping [Reynolds number (Re) < 1]. The Brinkman–Forchheimer model is essentially an extension of Darcy's model and is used when the flow regime is not creeping. In such cases, inertial effects in the porous medium must be considered.

2.2 Porosity

Porosity (ϵ) in porous media is defined as the fraction of the total volume occupied by pores. Consequently, $1-\epsilon$ represents the fraction occupied by the solid matrix. For homogeneous media, the surface porosity is equal to ϵ , meaning that a fraction of the total surface area is occupied by pores. This definition assumes that all pore spaces are interconnected. However, if this assumption does not hold, and the pores are isolated, effective porosity is defined as the ratio of the interconnected void volume to the total volume.

3. HEAT TRANSFER IN POROUS MEDIA: CONCEPTS AND TYPES OF CONVECTION

In general, the local temperature of the fluid and solid phases within a porous medium is not identical, a condition termed "local thermal nonequilibrium." Under such circumstances, energy equations are formulated independently for both the fluid and solid phases. This assumption is particularly relevant in scenarios involving high fluid velocities or in the presence of internal heat generation within the porous medium. Conversely, under the assumption of local thermal equilibrium, the average temperature of both phases is considered equal, and a single effective energy equation is employed. By systematically investigating the influence of various parameters such as Grashof (Gr), Darcy Da, and Reynolds numbers on velocity and temperature profiles, as well as exploring different boundary conditions, and porous media orientations, and comparing the heat transfer behavior under both local thermal equilibrium and nonequilibrium conditions in diverse geometries, it can be concluded that porous media enhance heat transfer.

Having established the concepts of thermal equilibrium and nonequilibrium in porous media, we can now delve into the various modes of heat transfer, including free convection, forced convection, and mixed convection.

3.1 Forced and Free Convection

Convection is a significant mode of heat transfer in nature, which occurs due to the movement of a fluid relative to a solid surface. When a fluid flows over a solid, heat transfer takes place between the fluid and the solid surface if there is a temperature difference. This heat transfer is facilitated by the fluid's motion relative to the solid.

Forced convection occurs when a fluid is forced to flow over a solid surface due to an external force, such as a pump or fan. The applied force induces fluid motion, resulting in heat transfer between the fluid and the solid surface.

Free convection occurs when temperature differences within a fluid body create density variations, leading to buoyancy forces. The buoyancy force, which is directly proportional to the density difference, drives the fluid motion. In free convection, the Gr is a crucial parameter that quantifies the relative magnitude of buoyancy forces (Holman, 1997).

In free convection systems, the Gr can be physically interpreted as a dimensionless group representing the ratio of buoyancy forces to viscous forces. This interpretation is analogous to the Re in forced convection systems and serves as the primary criterion for the transition from laminar to turbulent boundary layer flow. Mathematically, the Gr is defined as

$$Gr_x = \frac{g\beta\Delta Tx^3}{v^2},\tag{2}$$

where g is the gravitational acceleration, $T_w - T_\infty$ is the temperature difference, x is the characteristic length, v is the kinematic viscosity of the fluid, and β is the volumetric thermal expansion coefficient (Holman, 1997).

In free convection systems, the Rayleigh number (Ra) is a dimensionless parameter that quantifies the relative significance of buoyancy forces compared to viscous forces. It is defined as the product of the Gr and the Prandtl number (Pr):

$$Ra = Gr \times Pr = \frac{g\beta\Delta TL^{3}\rho}{\mu\alpha},$$
(3)

where μ is the dynamic viscosity of the fluid, α is the thermal diffusivity of the fluid, and Pr is the ratio of momentum diffusivity to thermal diffusivity.

Furthermore, k represents the thermal conductivity coefficient, and C_p denotes the specific heat coefficient at constant pressure. The dimensionless Nusselt number (Nu) is employed to quantify the heat transfer from a heated surface to the adjacent fluid. This number is defined as follows:

$$Nu = \frac{hL}{k},\tag{4}$$

where h is the heat transfer coefficient, L is the characteristic length, and k is the thermal conductivity coefficient of the fluid.

Generally, the combined effects of forced and free convection exist when $Gr_L/ReL^2 = 1$. If $Gr_L/ReL^2 \gg 1$, free convection is neglected, and conversely, when $Gr_L/ReL^2 \ll 1$, the effects of forced convection are negligible (Holman, 1997).

3.2 Mixed Convection

Mixed convection occurs when both forced and free convection mechanisms contribute to heat transfer. This typically happens in situations where a fluid flows at a low velocity over a heated surface. The buoyancy forces arising from the temperature-induced density differences augment the forced flow, leading to a complex interaction between the two convection modes. Mixed convection is characterized by the interaction of free and forced convection mechanisms, influencing both heat transfer and flow patterns. Buoyancy forces, arising from temperature-induced density differences, drive free convection. Conversely, forced convection is driven by externally applied forces. The Ra and Re are key parameters in the analysis of mixed convection phenomena. The Ra quantifies the significance of free convection, whereas the Re characterizes forced convection. The relative contributions of these two mechanisms to heat transfer and flow patterns can be assessed by comparing their respective values. Dominance of forced convection occurs when the Re substantially exceeds the Ra. Conversely, free convection prevails when the Ra significantly surpasses the Re. In cases where these numbers are of a similar order of magnitude, both mechanisms interact to influence the flow and heat transfer (Holman, 1997).

A multitude of techniques have been developed to enhance heat transfer in fluids. As depicted in Fig. 1, these methods can be broadly classified as active or passive. Passive methods encompass extended surfaces and additive fluids. Nanotechnology represents a significant advancement within the realm of additive fluids.

4. NANOTECHNOLOGY

The term "nanofluid" was coined by Choi and Eastman (1995) to describe a novel type of fluid consisting of a base fluid with a small amount of suspended metallic or nonmetallic nanoparticles. These nanoparticles are dispersed homogeneously and stably within the continuous phase. Early research and development in nanofluid technology demonstrated the significant potential of nanofluids for heat transfer applications.

Nanoparticles are particles with dimensions typically ranging from 1 to 100 nm. They can be composed of metals, insulators, semiconductors, or composite materials such as core-shell structures. Common shapes include nanospheres and nanorods. Smaller nanoparticles are categorized as nanoclusters. Nanocrystals and semiconductor quantum dots are also considered types of nanoparticles.

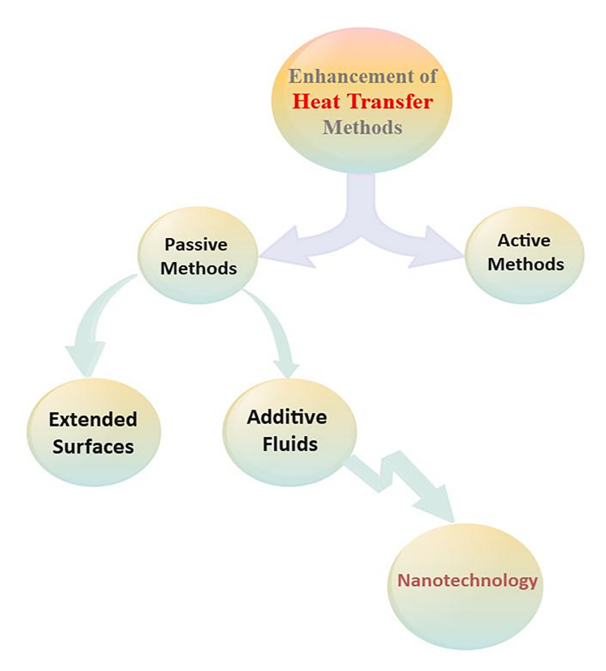


FIG. 1: Enhancement of heat transfer methods

Nanoparticles can be categorized into four primary types: elemental nanoparticles, ceramic oxide nanoparticles, carbon nanotubes, and mineral nanomaterials. Figure 2 provides a comprehensive visualization of this classification scheme.

There are numerous techniques available for the production of nanoparticles. These techniques can be classified into three primary categories. A schematic representation of these methods is provided in Fig. 3.

4.1 Heat Transfer Models in Nanofluids

The outstanding properties of nanofluids, such as enhanced thermal conductivity compared with traditional fluids, their relatively simple preparation, and acceptable viscosity, make them prime candidates for coolant applications. Conventional fluids exhibit significantly lower thermal conductivity compared with solids. Figure 4 illustrates the thermal conductivity of various common fluids and solids (metals and nonmetals). Clearly, solids possess higher thermal conductivity than conventional fluids.

5. PHASE CHANGE MATERIALS

Another effective method to enhance heat transfer is the use of phase change materials (PCMs). PCMs possess the ability to store thermal energy in two forms: sensible and latent heat. Sensible heat is stored as the temperature of a solid or liquid increases. The quantity of sensible heat stored within a substance is a function of its temperature, specific heat capacity, and mass. Latent heat storage occurs during phase transitions, such as solid-to-liquid, liquid-to-gas,

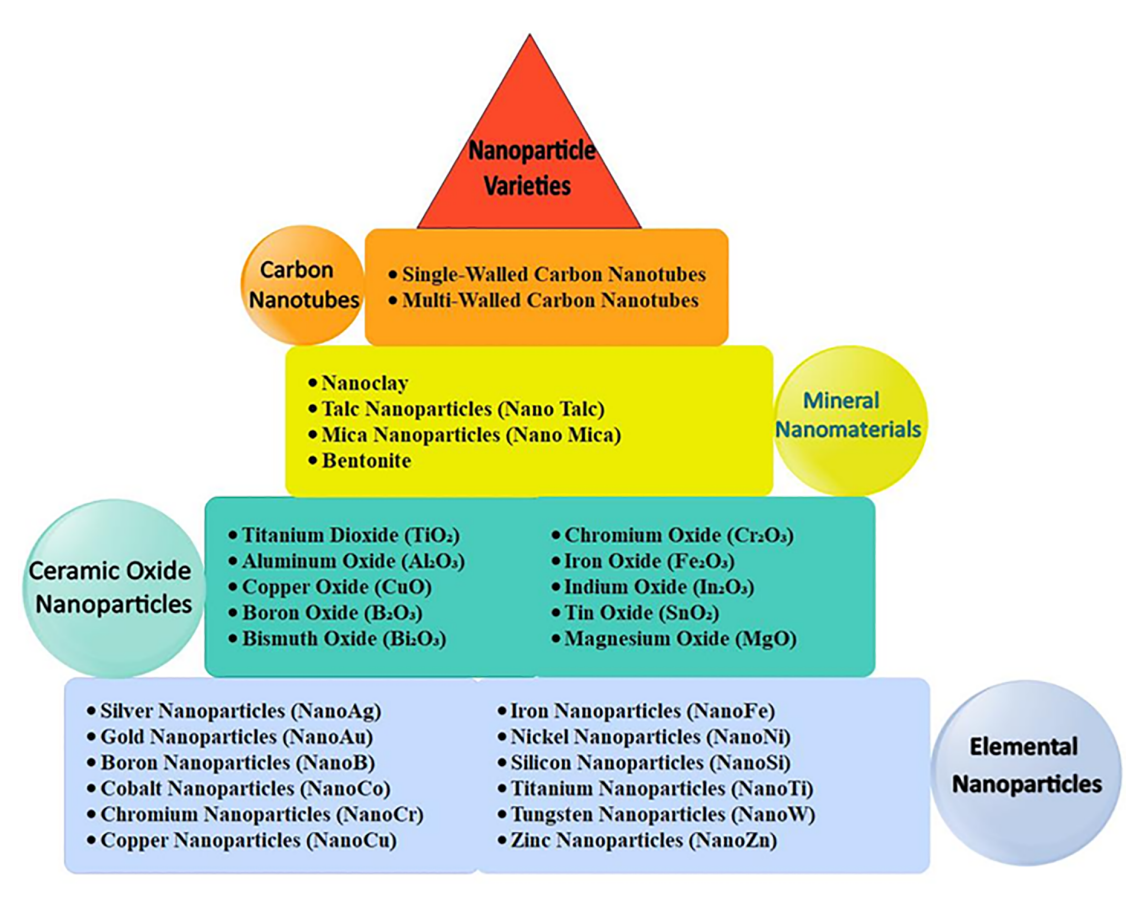


FIG. 2: Nanoparticle varieties

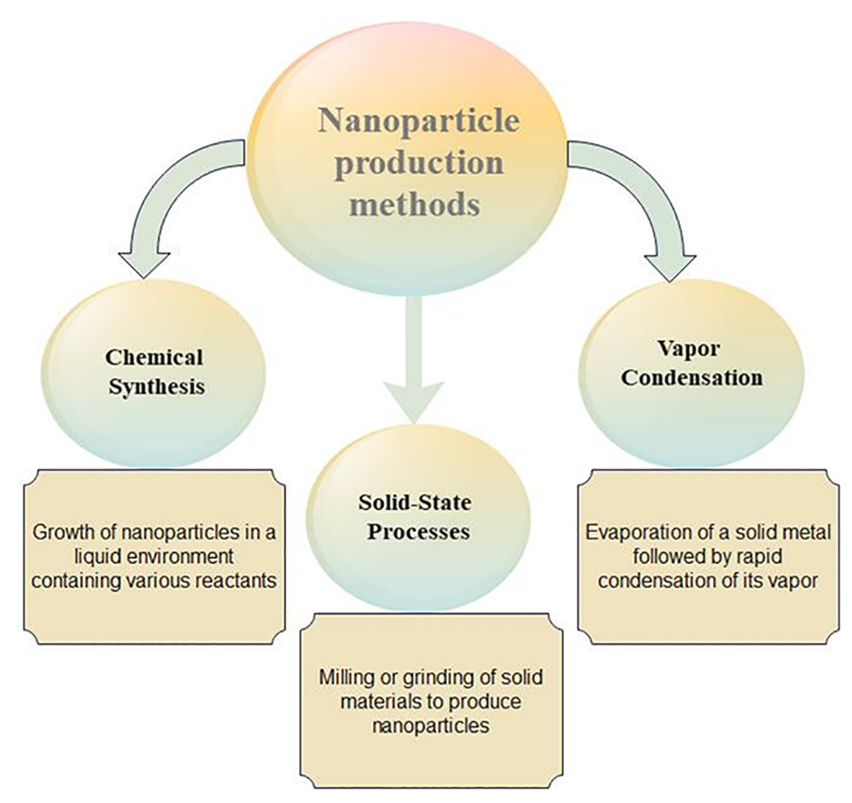


FIG. 3: Nanoparticle production methods

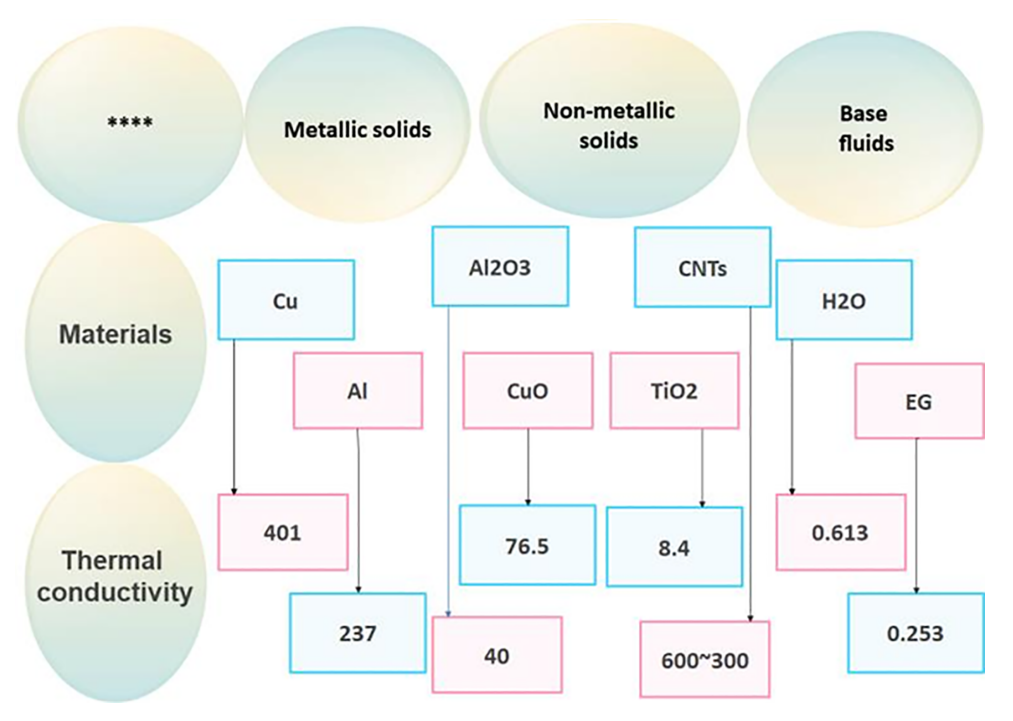


FIG. 4: Thermal conductivity coefficient of various substances

or solid-to-solid. PCMs primarily store energy in the form of latent heat of fusion (Mehling and Cabeza, 2008). Heat storage through phase change in various states is as follows:

Solid-solid phase transformations are not considered suitable due to the exceedingly slow rate and minimal quantity of heat transfer involved in such processes. Liquid—gas phase transformations are not feasible owing to the elevated thermal energy requirements and the concomitant generation of high-pressure gaseous phases. Solid—liquid phase transformations are more advantageous because phase change materials undergo a phase transition from a solid to a liquid state at a constant temperature upon absorbing latent heat, subsequently releasing this energy at approximately the same temperature. PCMs are in a solid state at ambient conditions. PCMs can be categorized into two primary divisions: organic and inorganic materials. A schematic representation of this classification is illustrated in Fig. 5.

5.1 Thermal Conduction Enhancement of PCMs

Despite their high density, the low melting and freezing rates of phase change materials can reduce the potential of energy storage systems in specific applications. This is because almost all conventional phase change materials have low thermal conductivity. In general, the thermal conductivity of phase change materials can be increased by using materials with a high conductivity coefficient. This increase in thermal conductivity can be achieved through various methods:

- Saturation of porous materials with high thermal conductivity in PCMs
- Dispersion of high-thermal-conductivity particles in PCMs
- Embedding of metallic compounds and structures in PCMs
- Use of materials with high thermal conductivity and low density

Although the incorporation of graphite composites into PCMs can enhance system efficiency, it is limited by the time-consuming and costly production process. The addition of micro- and nano-sized high-thermal-conductivity particles to PCMs improves their thermodynamic properties and results in increased system performance (Jegadheeswaran and Pohekar, 2009).

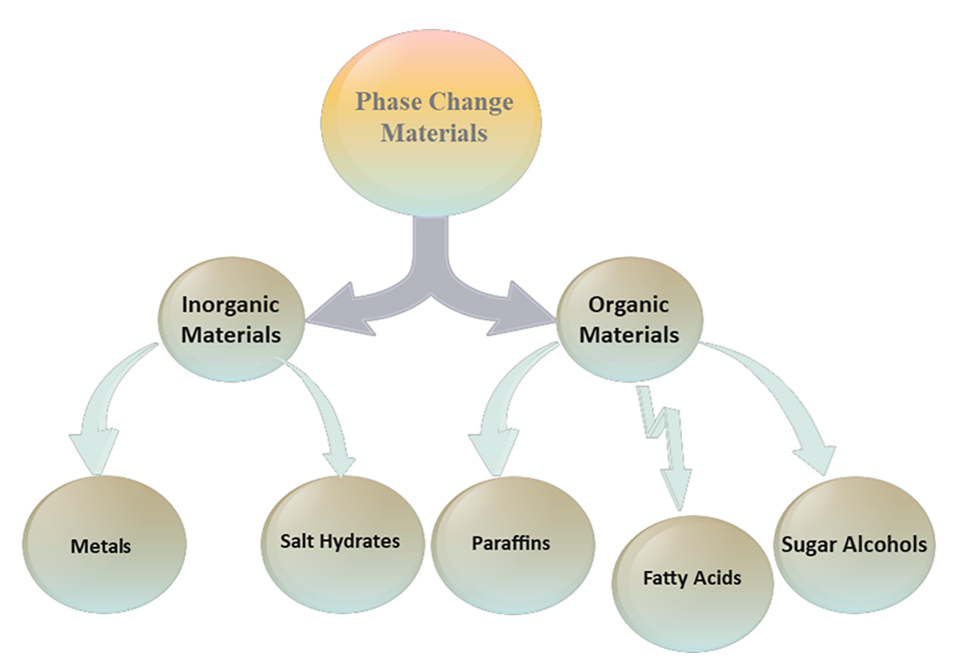


FIG. 5: Classification of phase change materials

6. RESULTS AND DISCUSSION

Numerous studies have been conducted on heat transfer in porous media using nanofluids. Among these, comprehensive reviews play a pivotal role in advancing the scientific and practical goals of this field. Nabwey et al. (2023) provided a comprehensive review of nanofluid heat transfer in porous media, meticulously evaluating all published research up to 2020. Their novel analytical approach introduced a new parameter (Azizimehr et al., 2024) that strongly correlates with heat transfer processes and enhances the performance of existing systems (Moltames et al., 2019). Building on Nabwey et al.'s (2023) work, this section aims to conduct a more comprehensive and in-depth review of research published since 2020 on nanofluid heat transfer in porous media. This review focuses on the advancements in PCM technology and the combination of nanoparticles with PCMs (NPCMs).

6.1 Integrated Free Convectional Heat Transfer

Hussain et al. (2022) investigated free convection heat transfer in a corrugated enclosure filled with a non-Newtonian hybrid nanofluid. Their numerical results indicated that the highest heat transfer rate was achieved for a pseudoplastic hybrid nanofluid with a high Ra and low thermal conductivity ratio and Hartmann number (Ha). In another study, Armaghani et al. (2024) examined free convection heat transfer in a tilted porous corrugated hybrid enclosure filled with a nanofluid under the influence of a magnetic field. Their findings revealed that increasing the nanofluid's volumetric friction resulted in a higher average Nu and heat generation rate. Nazarahari et al. (2024) experimentally investigated free convection heat transfer of nanofluids in porous media with various pore shapes. Their results showed that the highest heat transfer coefficient and Nu were achieved for nanofluids at a 30° angle with a square porosity, whereas the lowest values were recorded at 0°. Hashemi et al. (2024) numerically studied three-dimensional unsteady free convection of Al₂O₃—water nanofluids using a vibrating plate with the two-way fluid-structure interaction technique. Their results indicated that a vibrating plate closer to the right side of the cavity increased the heat transfer coefficient. Additionally, increasing the width of the vibrating plate also had a positive impact on the heat transfer coefficient. Table 1 presents a comparison of recent studies (2020—present) on the free convection of nanofluids in porous media, considering parameters such as methodology, nanofluid type, geometry, and decision variables.

6.2 Forced Convectional Heat Transfer

Ghasemiasl et al. (2023) conducted a comprehensive review of the forced convection of nanofluids in channels and tubes. They initially introduced the types of flow and the governing equations and then performed a comprehensive comparison in terms of methodology, type, and size of nanoparticles, nanoparticle volume fraction, and flow conditions. Soleymani et al. (2022) numerically investigated turbulent flow, heat transfer, and entropy generation of a water-based magnetic nanofluid in a tube with a porous hemisphere under a uniform magnetic field. They demonstrated that the Nu decreased to a minimum value as porosity reached 0.8. The increase in heat transfer was more effective with increasing the Ha compared with adding nanoparticles. A higher Ha and larger volume fraction of nanoparticles resulted in broader performance evaluation criteria. Table 2 presents a comparison of recent studies (2020–present) for forced convection of nanofluids in porous media, considering the aforementioned parameters.

6.3 Mixed Convectional Heat Transfer

Rashad et al. (2021) investigated magnetohydrodynamic (MHD) mixed convection in a hybrid Al₂O₃-Cu-water nanofluid within an L-shaped cavity. Their results indicated that the maximum sink strength led to the best heat transfer performance. Hussain et al. (2023) analyzed MHD mixed convection and entropy generation of a non-Newtonian hybrid nanofluid in a new corrugated-wall elbow cavity with a fourth circular hot block and a rotating cylinder. Results showed that the Nu increased with increasing power-law index. Additionally, the heat transfer rate increased with increasing aspect ratio. Nemati et al. (2023) calculated the lattice Boltzmann method entropy generation of hybrid nanofluids under the influence of different magnetic field types. Their results showed that increasing

TABLE 1: Research paper characteristics related to the free convection heat transfer

Ref.	Geometry description	Nanofluid	Methodology	Results	Decision variables
(Agrawal et al., 2021)	Stretching surface	γ -Al ₂ O ₃ water- ethylene	Free Marangoni convection; MHD; thermal radiation	↑m, k→↓ velocity curve γ-Al ₂ O ₃ -H2O temp profile > γ-Al ₂ O ₃ -C ₂ H ₆ O ₂ NF	0.5 < K < 1.5 $0.05 < \phi < 0.2$
(Martin et al., 2021)	Vertical finned cylindrical antenna	Water– copper	Free convection, SIMPLE algorithm, Darcy-Brikman	fratio of thermal conductivities and nanofluid's volume $\rightarrow \uparrow Nu$. The correlation allows for Nu in 2.35 × $10^5 - 5.13 \times 10^7$ Ra	$2.35 \times 10^5 \le \text{Ra} \le 5.13 \times 10^7$; $0\% \le \text{friction varies} \le 5\%$; $4\le \text{ratio between the conductivity}$ of the porous material and of the water ≤ 41.2 ; $0 \le \varphi \le 5\%$; $Nu_L = 0.104 Ra_L^{0.317}$
(Miles and Bessaih, 2021)	Cylindrical annulus filled	Al ₂ O ₃ —water nanofluid	Free convection	$ ^{\uparrow} Nanoparticles \rightarrow ^{\uparrow} Nu, Da, porosity \\ effect; ^{} \uparrow Da, \epsilon \rightarrow ^{\uparrow} Nu, St; ^{\downarrow} St, Be \rightarrow ^{\uparrow} Nu $	$10^{3} \le Ra \le 10^{5}$ $10^{-4} \le Da \le 10^{-1}$ $0.2 \le \varepsilon \le 0.99$ $0 \le \varphi \le 0.08$
(Bairi, 2021)	Vertical concentric cones	Water– copper nanofluid	Free convection; SIMPLE	↑Heat transfer→↑volume friction of water-based copper nanofluid inc	$3.32 \times 10^5 \le Ra \le 6.74 \times 10^7$ $0 \le Nu \le 100$
(Mehryan et al., 2020)	Square cavity	Polyethene/ nano decane- water nanofluids	Free convection; Bongiomo's mathematical model; Darcy–Brinkman	Maximal heat transfer rate→highest volume fraction	$0\% \le \varphi \le 5\%$ $0.2 \le Stefan number \le \infty$ $0.2 \le volume fraction \le 0.6$ Pr = 6.2 $Ra = 10^6$ $\epsilon = 0.8$ $Da = 10^{-2}$
(Amine et al., 2021)	Triangular cavity and a circular porous media at its angled corner	Ag/Mgo– water hybrid nanoffuid	Free convection; Darcy–Brinkman's– Forchheimer equation	\uparrow Ra \rightarrow \uparrow heat transfer and \uparrow dissipation withen the cavity; \uparrow porous media thickness \rightarrow \uparrow Nu _{avg}	$10^{3} \le Ra \le 10^{6}$ $0 \le Ha \le 80$ $10^{-5} \le Da \le 0.15$ $0.1 \le \varepsilon \le 0.9$ $0 \le Nu_{\text{avgavg}} \le 1.8$ $10^{-5} \le \varphi \le 0.08$
(Esfe et al., 2022)	V-shaped enclosure	Al ₂ O ₃ -H ₂ O	Free convection, SIMPLE, Boussinesq	$ \uparrow Nu_{avg} \rightarrow \uparrow Ra, conv \ thermo-dominated; \\ \uparrow Nu_{avg} \rightarrow \uparrow \phi; \ \uparrow Thermal \ conductivity \rightarrow \uparrow Da $	$10^{-3} \le Ra \le 10^6$ $1.116 \le Nu_{\text{avg}} \le 8.828$ $0 \le Da \le 60$ $0\% \le \varphi \le 3\%$

	IABLE I: (connuuea)				
(Wang et al., 2022)	Micro- channel heat sink	MWCNT- Fe ₃ O ₄ hybrid nanofluid	Free convection; FVM; Darcy— Brinkman— Forchheimer; SIMPLE	↑CPU surface temp→↑heat transfer; ↑porous heat sink efficiency→↑CPU's performance	Re = 1000 Heat flux = 138 w/m^2
(Abderrahmane et al., 2022)	Inclined half-annulus porous enclosure	Al ₂ O ₃ -water	FEM; MHD; free convection; GFEM; Darcy–Brinkman– Forchheimer	For low Ra→boundary force is very slow; ↑Nu→↑Ra	$10^3 \le \text{Ra} \le 10^6$ $0 \le \text{Ha} \le 100$ $10^{-5} \le \text{Da} \le 10^{-4}$
(Tan et al., 2023)	Inclined porous annulus	$\mathrm{Ag-TiO}_2$	Free convection; Darcy–Brinkman– Forchheimer model	↑Ha → ↓heat transfer; ↑φ → ↓heat dissipation	$10^{-5} \le Da \le 10^{-1}$ $0 \le Ha \le 50$ $0 \le Q \le 20$
(Tayebi et al., 2023)	Porous inclosure with curved hot wall	Mixture of aluminum— water	Free convection; CVFEM; Darcy model; FVM; FEM	↑\$\phi\$ → ↑thermal feature of working fluid; The dispersion of nanoparticles→↑speed nanofluid; ↑Ha→↓free convection; ↑Ra→↑strength of vortex	$0 \le \text{Ha} \le 20$ $150 \le \text{Ra} \le 700$ $\Phi = 0.04$
(Kodi et al., 2023)	Wavy porous cylinder	Al ₂ O ₃ -water	Free convection; MHD; Darcy— Brinkman— Forchheimer	\uparrow Ra(to 10 ⁴) \rightarrow \uparrow thermal boundary forces; \uparrow Le \rightarrow \downarrow thermal boundary layer thicknesses; \uparrow Heat and mass transfer \rightarrow \uparrow Ra,Da, ϵ and \downarrow Ha,Le	$15 \le Ha \le 30$ $10^4 \le Ra \le 10^5$ $0.1 \le Le \le 10$ $Da = 10^{-3}$ $\epsilon = 0.5$
(Alilat et al., 2023)	Long vertical stretchable plate	Salty Reiner– Philippoff nanofluid	Free convection; Darcy–Forchheimer; electromagnetic radiation	↑Fr→↓velocity field; ↑nanofluid drag coefficient→↓speed range; ↑porosity→↓sheer stress, temp, concentration	$Pr = 6.2$ Sc = 4 $0\% \le \phi \le 3\%$ $3.32 \times 10^{5} \le Ra \le 6.7 \times 10^{7}$
(Girish et al., 2023)	Conical gap	Cu-water	Free convection; Brinkman model; Maxwell model	When the cone is tilted→↑heat transfer; when the cone is tilted→heat transfer being max	$0\% \le \varphi \le 5\%$ 3.32 × $10^5 \le \text{Ra} \le 6.7 \times 10^7$ $\epsilon = 0.99$
(Hosseinzadeh et al., 2023)	Permable fin	Hybrid nanofluid	Free convection; differential transformation method	↑Nr, Nc→†thermal distribution; ↑convective factor→↓temp of fin; ↑Nc→↑Da; ↑Ra→↓thermal resistance	$0.5 \le Sp \le 1.5$ $0 \le Q \le 0.4$ $0.5 \le Nc \le 1.5$ $2 \le Nr \le 6$
(Reddy et al., 2023)	Wavy, porous, starlike enclosure	Fe ₃ O ₄ /Al ₂ O ₃ -1-hexanol	Free convection; MHD; GFEM; Taguchi method; RSM; Darcy law	↑porosity→is detrimental in conv mode of thermal evolution; ↑Ha→↓nanofluid recirculation within the bounded wavy encloser	$10 \le \text{Ra} \le 100$ $0 \le \text{Ha} \le 25$

TABLE 1: (continued)

Ref.	Geometry description	Nanofluid	Methodology	Results	Decision variables
(Salehi et al., 2023)	Porous wavy stretching surface	TiO ₂ —water	Free convection; Darcy–Brinkman; FEM	↑Ra→↑max streamline number	$10^3 \le \text{Ra} \le 10^5$ $0 \le \text{Ha} \le 10$ $2\% \le \Phi \le 4\%$ Da = 0.01
(Habibishandiz et al., 2023)	Square cavity		Free convection; Darcy–Brinkman	$\uparrow \text{Microorganism} \rightarrow \downarrow \overline{\textit{Nu}}_{\text{av}} \text{ (in T = cte);}$ $\uparrow \text{Ra, Pe} \rightarrow \downarrow \overline{\textit{Nu}}_{\text{av}} \text{ (T = cte);} \uparrow \text{Bio conv}$ $\text{Le} \rightarrow \downarrow \text{flow strength}$	$0 \le Ra \le 100$ $0 \le Rd \le 3$ $10 \le Rd \le 100$ $1 \le Ln \le 10$ Le = 1 $\delta = 1$
(Al-Amir et al., 2023)	Porous titled z-staggered cavity	TiO ₂ –water	Free convection; Darcy–Brinkman; FEM	↑Da, Ra \rightarrow ↑upper and lower cavity heat transfer coefficient; $\uparrow \phi \rightarrow \uparrow$ heat transfer	$10^3 \le Ra \le 10^6$ $10^{-5} \le Da \le 10^{-1}$ $0 \le \phi \le 0.1$
(Liu et al., 2024)	Infinite vertical porous media	Cu-water	Free convection; MHD		$0.1 \le \varphi \le 0.4$ $0 \le Q \le 150$
(Mandal et al., 2024)	Porous wavy enclosure	Al ₂ O ₃ /Cu– water	MHD; free convection	$\uparrow Da, Ha \rightarrow \downarrow Nu_{av}; \downarrow Nu_{av} \rightarrow \uparrow \phi, \epsilon$	$0.4 \le \epsilon \le 1$ $0 \le \phi \le 0.05$ $10^{-3} \le Da \le 10^{-1}$ $0 \le Ha \le 70$ $2.742 \le Nu \le 12.35$ $Ra = 10^5$
(Ghali et al., 2022)	Symmetrical cavity with two semicylinders	$Fe_3O_4/MWCNT-$ water	Free convection; G_FEM	↓Da,Ha,Ra → ↑ porosity,↓φ; ↑heat transfer, ↑Ha→↑Da, Ra, φ;	$10^3 \le Ra \le 10^6$ $10^{-5} \le Da \le 10^{-2}$ $0.02 \le \phi \le 0.08$ $0.2 \le \epsilon \le 0.8$ $0 \le Ha \le 100$
(Abbas et al., 2023)	Vertical	Cu/Ag/TiO ₂ — water	MHD; free convection; FDM; CGM	↑chemical reaction parameter→↓concentration profile Cu-nanofluid→most appropriate for enhancing the mechanical properties; TiO₂-nanofluid→best type for reducing the surface shear stress	$\begin{aligned} & \text{Pr} = 1.5 \\ & \text{Ec} = 0.3 \\ & \text{Sc} = 1.2 \\ & 0 \le \phi \le 0.1 \end{aligned}$

TABLE 1: (continued)	tinued)				
(Khalili et al., Square 2024) cavity	Square cavity	Cu-water	Free convection; lattice Boltzmann method	$\uparrow Ra \rightarrow \uparrow \text{free convection; } \uparrow Gr \rightarrow \uparrow \phi;$ $\uparrow \phi \rightarrow \uparrow Nu_{av}$	$0.05 \le \varphi \le 0.2$ $3 \times 10^6 \le \text{Ra} \le 3.5 \times 10^5$ $10^3 \le \text{Gr} \le 10^5$ Pr = 6.2
(Sajjadi et al., 2024)	Porous cavity with horizontal fins	Cu-water	Free convection; lattice Boltzmann method	↑Porosity of porous cavity→↑Nu _{av}	$10^{-4} \le Da \le 10^{-2}$ $10^3 \le Ra \le 10^5$ $0.4 \le \epsilon \le 0.9$

TABLE 2: Research paper characteristics related to the forced convection heat transfer

Ref.	Geometry description	Nanofluid	Methodology	Results	Decision variables
(Soleymani et al., 2022)	A tube with hemisphere porous	Fe_3O_4 -water nanoffuid	Force convection; Darcy-Brinkman's equation; SIMPLE; MHD	$\uparrow NU \longrightarrow \uparrow Re$, \uparrow nanoparticle, $\uparrow \phi$, \uparrow Ha, \downarrow porous media; max $NU \longrightarrow when Re = 25,000, \epsilon = 0.2, Ha = 50$	$50 \le \text{Nu} \le 310$ $1000 \le \text{Re} \le 25000$ $0.2 \le \varepsilon \le 0.8$ $0 \le Ha \le 50$ $0 \le \varphi \le 0.025$
(Wang et al., 2021)	Porous twisted tape tube (round and triangular)	Silica-water (SiO ₂ -H ₂ O)	Force convection; SIMPLE algorithm	↑Mass friction and porous twisted tape →↑ Nu, flow resistance coefficient	$0 \le Nu \le 300$ $6000 \le \text{Re} \le 36000$ $0 \le f \le 0.07$ $0 \le \Delta P \le 300$
(Saghir et al., 2020)	Aluminum metallic foam	Water-aluminum nanofluid	Force convection; Darcy–Brinkman	→Force convection →↑heat; ↑permeability→↑heat	$\%0.1 \le concentration \le \%0.5$
(Arafa et al., 2022)	Curved vertical channel	Nonhomogeneous peristaltic nanofluids	Force convection; Darcy–Brinkman; Boltzmann	†dissipation coefficiant $\rightarrow \uparrow G(y)$, $\phi(y)$, $u(y)$; $\uparrow Q \rightarrow \uparrow$ peristaltic convective transport	†Dissiption coefficient $\rightarrow \uparrow \theta(y)$, $\phi(y)$, $u(y)$, Pr = 4.623, $\delta = 155$, Le = 2.62×10^5 , $\%0 \le Q_{av} \le 5\%$
(Sivasankaran and Bhuvaneswari, 2022)	Double pipe heat exchanger with a counter flow	TiO ₂ /Al²O ₃ -water	Turbulent forced convection; Darcy– Brinkman mode	$\uparrow Q \rightarrow \uparrow$ peristaltic convective transport (owing to increased temperature difference)	$0.1 \le Gr \le 0.3$ $\%0 \le Q_{av} \le \%5$ $-2 \le Q \le 3$ $Pr = 4.623$ $\delta = 155$
(Aminian et al., 2020)	Corrugated mini- channel (wavy channel)	Al ₂ O ₃ /CuO–water	Force convection; Darcy-Brinkman- Forchheimer	↓Da→↑Nu _x from 0.1 to 0.0001; ↓friction factor→↑Da from 0.1 to 0.0001 highest Nu state for Al ₂ O ₃ (for thermophysical characteristics)	$0.00001 \leq Da \leq 0.1$

Re decreased the effect of increasing Ha on the average Nu. Mansour et al. (2024) evaluated the MHD unsteady mixed convection heat transfer of a hybrid nanofluid in a corrugated porous cavity with thermal radiation. Their results showed that as the heat source length and the number of waves in a porous medium with a hybrid nanofluid (TiO₂–Ag/water) increased, the average Nu increased. Moreover, increasing the nanoparticle volume fraction and porosity improved heat transfer, while increasing the Ha decreased the average Nu. Table 3 presents a comparison of recent studies (2020–present) for mixed convection of nanofluids in porous media, considering the aforementioned parameters.

6.4 Other Research on Nanofluid Heat Transfer in Porous Media

Li et al. (2021) investigated the heat and mass transfer of a MHD nanofluid flow on a porous stretching. Their results showed that as the Brownian motion parameter increased, the heat transfer rate was reduced. On the other hand, a higher thermophoretic parameter led to a higher heat transfer rate. As Pr and Lewis number increased, Sherwood's number was also augmented. Farahani et al. (2021) investigated the influence of a magnetic field on heat transfer from a channel with nanofluid flow and a porous layer configuration. Their results showed that the heat transfer rate was higher in the central arrangement compared with the boundary arrangement. When the dimensionless thickness of the porous medium in the central arrangement was 0.8, the heat transfer rate was at its peak. Conversely, the minimum heat transfer rate occurred when the dimensionless thickness in the boundary arrangement was set to 0.6. Table 4 presents a comparison of recent studies (2020–present) for heat transfer of nanofluids in porous media, considering the aforementioned parameters.

6.5 Overall Review of Papers

The primary objective of adding nanoparticles to a base fluid is to enhance heat transfer. Udoh et al. (2024) conducted a study to enhance the performance of anticorrosive coatings by incorporating a base nanofluid into coatings with a porous matrix, allowing for controlled release and self-healing capabilities. Porous matrices can improve heat transfer; therefore, the base nanofluids within these matrices not only aid in corrosion protection but also enhance the thermal properties of the coatings. Memon et al. (2023) found that adding a base nanofluid (CuO–H₂O) to a porous medium significantly affects heat transfer. Increased nanoparticle concentration improves the Nu and heat transfer efficiency, whereas higher porosity of the nanofluid reduces the Nu and decreases heat transfer performance. Farahani et al. (2023) investigated the thermal performance of microchannel heat sinks. Their study shows that incorporating nanoparticles into water and PCMs can reduce thermal resistance (R) and increase the thermal performance enhancement factor (TPEF). In particular, combining PCM with aluminum oxide and iron oxide nanoparticles provides the greatest improvement in TPEF. Additionally, using a porous medium alongside PCM can reduce thermal resistance by approximately 60% and enhance thermal performance. Table 5, a summary of Tables 1 through 4, presents the increase in the Nu in nanofluids under various conditions, including different volume fractions, Re, Ra, and Da. From this table, the following can be inferred:

- The Nu exhibited a significant enhancement with increasing Ra and nanoparticle concentration. For instance, at the highest Ra value, the Nu improved by up to 65%.
- For an Ra of 10⁵, the Nu for a silver-water nanofluid increased by as much as 9.5%.
- Adding nanoparticles improved the Nu by up to 21%.
- In a triangular tube with a Re of 13,000, the Nu increased by 54.83%.
- For a Ra of 10⁵ and a nanoparticle concentration of 0.05%, the Nu reached 9.76.
- For the Da of 10^{-4} , the Nu varied between 1.25 and 7.0.
- The Nu increased with an increase in the Gr from 150 to 450.
- The Nu was observed to decrease by up to 50.48% with increasing Ha.
- The Nu improved by 20% to 70% as different nanoparticles were added.

Hence, higher nanofluid concentrations and Ra are correlated with substantial enhancements in the Nu. Conversely, as the Ha increases, the Nu tends to decrease.

TABLE 3: Research paper characteristics related to the mixed convection heat transfer

Ref.	Geometry description	Nanofluid	Methodology	Results	Decision variables
(Alghamdi et al., 2021)	Structure bounded by a vertical elongating slender concaved-shape	Sodium alginate– based nanofluids	Darcy–Brickman; GDQLIM; KBM; MHD; mixed convection	$\downarrow \phi \to \downarrow \text{velocity;} \uparrow Q \to \uparrow \phi, M, A, B$	$0<\phi<0.2$
(Bakar et al., 2021)	Porous medium with heat generation	Ag/TiO ₂ . H ₂ O hybrid nanofluid	MHD; mixed convection	↑Skin friction coefficient and velocity profile—nanoparticles of HNF ↑0% /10 and condition of porous martial and base fluid varies between 4/41.2	$0 \le \eta \le 20 - 0.2$ $\le f(\eta) \le 1$
(Jakeer et al., 2021)	Lid-driven porous cavity	Cu-Al ₂ O ₃ —water hybrid nanoffuid	Mixed convection; Cattaneo-Christov heat flux pattern; SIMPLE	\uparrow Da → ↑velocity and heat transfer rate; HNF, λ > CuAl ₂ O ₃ -water NF; Ha → ↑thickness of the right wall and Nu	$0.1 \le Ri \le 100$ $0.1 \le Ha \le 100$ $0.1 \le Re \le 25$ $10^{-2} \le Da \le 10^{-6}$
(Yeasmin et al., 2022)	Lid driven L-shaped cavity	Kerosene–alumina nanofluid	Mixed convection; Darcy-Brinkman equation	↑Porous media→†Da	$10^{-4} \le Da \le 10^{-2}$ $0.1 \le \tau \le 1$ $\delta = 0.05$ $0.1 \le Ri \le 100$
(Khan et al., 2022)	Porous vertical cylinder	Al ₂ O ₃ -Cu-water	Mixed convection; Darcy–Brinkman	↑Drag force→due to radiation and curvature parameters, ↓velocity→due to heat source/sink and radiation parameter	$Pr = 1$ $3 \le \epsilon \le 10$
(Sedki, 2022)	Nonliner permeable stretching surface	Water and oil— Cu, Al ₂ O ₃ , ZnO, Ag, SiO ₂	MHD; mixed convection; Darcy– Brinkman model	↑Skin friction coefficient→↑chemical reaction, thermal radiation, mixed convection, porous media; ↑Heat transfer→↑Brownian motion, chemical reaction	$\Phi = 0$ $0.72 \le Pr \le 10$ $0 \le Rc \le 0.8$ $0 \le Rd \le 12$
(Alsedais et al., 2022)	Undulating cavity containing obstacle	Cu-water	Mixed convection; FVM; Darcy— Brinkman; SIMPLE		$0.4 \le \epsilon \le 0.9$ $10^{-5} \le Da \le 10^{-1}$ $0 \le \phi \le 0.1$ $-2 \le Q \le 2$ $10 \le Ha \le 100$

TABLE 3: (continued)	inued)				
(Habibishandiz and Saghir, 2022)	(Habibishandiz Vertical annular and Saghir, porous cylinder 2022)	Nanofluid containing oxytactic micro- organism	MHD, mix convection; FVM; Darcy momentum conservation equation	Presence of microorganism $\rightarrow \downarrow q''$; \uparrow Ha $\rightarrow \uparrow$ heat transfer; \uparrow Re, $\stackrel{\text{Pr}}{\rightarrow}$, Le $\rightarrow \uparrow$ heat transfer; \uparrow Ln, Rb, Pe $\rightarrow \downarrow Nu$	Re. Pr = 10 $10 \le \frac{\text{Ha}}{10} \le 100$ $10 \le Nu \le 25$ $1 \le \text{Pe} \le 10$ $1 \le \text{Le} \le 10$
(Al Qarni et al., 2023)	Vertical core with porous matrial	Maxwell nanoffuid	Darcy–Fochheimer– MHD; Bongiorno model; mixed convection	↑Temp→↑radiation, thermophoresis; ↓velocity→↑Maxwell parameters and magnetic parameters	$0.2 \le Pr \le 2.4$ $0.2 \le Du \le 0.6$ $0.2 \le Le \le 1$ $0.1 \le Rd \le 0.9$ Sc = 4
(Jiang et al., 2023)	Cubic porous cavity with wavy wall and rotating cylinders	Fe ₃ O ₄ /MWCNT– water hybrid nanofluid	Mixed convection; MHD; GFEM; Forchheimer–Darcy model; FEM	↑Ha→↓velocity magnitude,↓Nu; ↑Da→↑Nu (especially at the ↓Ra);	$0 \le \text{Ha} \le 10$ $10^{-5} \le \text{Da} \le 10^{-2}$ $0 \le \phi \le 0.04$
(Maneengam et al., 2022)	Trapezoidal porous enclosure	Hybrid nanoffuid	Mixed convection; MHD	\uparrow Fluidity of the fluid $\rightarrow \uparrow$ Da, rotating velocity of inner tube; \uparrow Ha $\rightarrow \downarrow$ flow motion; \uparrow concentration of nanoparticles $\rightarrow \uparrow$ thermal conductivity; \uparrow Nu _{av} $\rightarrow \downarrow$ Ha; \uparrow domination of forced convection $\rightarrow \uparrow$ Nu _{av}	$0\% \le \varphi \le 6\%$ $10^{-5} \le Da \le 10^{-3}$ $0 \le Ha \le 100$
(Sajjadi et al., 2024)	Porous media	Non-Newtonian slippery nanofluid	Mixed convection; MHD	Slip velocity parameter ~ skin friction coefficient, Nu, Sh	$\begin{aligned} Pr &= 3 \\ Le &= 1 \\ E &= 0.2 \end{aligned}$

TABLE 4: Research papers related to other research on heat transfer

Ref.	Geometry description	Nanofluid	Methodology	Results	Decision variables
(Li et al., 2021)	Exponentially porous stretching	Williamson nanoffuid	MHD	The temp rise with scaling up Pr, $Q \uparrow N_b \rightarrow Nu \downarrow \uparrow Sh \rightarrow \uparrow Pr, Le$	1.5 \le Pr \le 2.4 0 \le Q \le 1.5 0.5 \le Le \le 2 0 \le k \le 3
(Farahani et al., 2021)	Circular channel	Cu-water	Horkheimer's porous media flow; Darcy– Brickman; FVM	↑φ→↑ heat transfer,↑ average convective heat coefficient; ↓Darcy number→↑ Nu	$0.5 \le \text{volume friction}$ ≤ 1 $0 \le \text{darcy number} \le 1$ $0 \le \text{magnetic flied} \le 1$
(Rashed et al., 2021)	Cubic enclosures filled	Non- homogenous two-phase Buongiorno's nanofluid	SIMPLE, Darcy model	↓Da→↓iso-surfaces temp, φ ,↑heat transfer coefficient; ↑ $Ra\rightarrow$ ↑ Convection process, temp, φ , heat transfer coefficient	$\begin{aligned} &10^4 \leq Ra \leq 10^6 \\ &0.01 \leq \phi \ 0.03 \\ &10^{-2} \leq Da \leq 10^{-4} \\ ⪻ = 4.623 \end{aligned}$
(Meghdadi Isfahani, 2017)	Micro-/nano- channel filled with porous media	Micro/ Nanoflows	Lattice Boltzmann method; Darcy's law; convection	Min Knudsen→ at $Kn = 0.1$; ↑Da→↑ Knudsen number	$0.732 \le \varepsilon \le 0.897$ $10^{-2} \le Kn \le 10^{2}$ $0.1 \le Nu \le 7$
(Rana et al., 2021)	Exponentially elongated porous plate	Magneto-nano micro polar liquid	Two-component Buongiorno model		$3 \le Sc \le 5$ $0.1 \le Nb \le 0.5$ Ec = 0.1, 5 Nt = 0.2
(Hasnain et al., 2022)	A long-infinite horizontal composite channel	Cu/Cuo-H ₂ O; Co/Al ₂ O ₃ -H ₂ O	Darcy–Brinkman model; FEM; MHD; Cattaneo– Christov heat flow model	↑Suction velocity→↓velocity of fluids, ↑Ha→↓velocity profile	$\begin{split} \epsilon &= 0.01 \\ \mu &= 0.5 \\ C_{r} &= 0.5 \\ P_{r} &= 7 \\ E_{c} &= 0.5 \end{split}$
(Hussain and Sheremet, 2022)	A vertical stretching surface	CNTS-water	Darcy–Brinkman– Forchheimer model; Buongiorno nanofluid model	↑Nanoparticle concentration → ↑thermal profile of NF; ↑Ri, Da → ↓temp profile	$0.1 \le Ri \le 10$ $0.01 \le Da \le 0.08$ Pr = 6.2 $0.01 \le Ec \le 0.04$ $0 \le Ha \le 1.5$ $0.5 \le \varepsilon \le 0.9$ $0 \le \varphi \le 0.06$

TABLE 4: (continued)	inued)				
(Sadighi et al., 2022)	Porous stretching cylinder	Fe ₃ O ₄ -water	MHD; Darcy–Brinkman model; Frobenius method	↑φ and curvature→local skin fraction coefficient	$Pr = 6.2$ $Sc = 0.62$ $1 \le Ha \le 4$ $0.01 \le Da \le 0.1$ $0.01 \le \phi \le 0.03$ $Ra = 4$ $Q = -5$
(Abderrahme et al., 2022)	An annulus enclosure	Carboxy-methyl/cellulse-Al ₂ O ₃	Darcy–Brinkman– Forchheimer; MHD; GFEM	↑Skin friction coefficient→↑thermal radiation, mix conv, porous media, magnetic field, Brownian motion	$10^3 \le Ra \le 10^6$ $0 \le Ha \le 100$ $10^{-5} \le Da \le 10^{-2}$ $\%0 \le \text{volume fraction}$ $\le \%8$
(Sultana et al., 2022)	Stretchable rotating disk	Carbon–water	Keller-box method; shooting method; Newton-Raphson method	†Volume fraction and $\phi \rightarrow \uparrow$ skin friction; ↑Pr \rightarrow †thermal boundry layer and temperature; ↓Nu \rightarrow ↑Pr, δ ↑porosity \rightarrow ↓Nu	$Pr = 6.2$ $0 \le \phi \le 0.2$
(Alilat et al., 2023)	Conical gap	Cu-water	Brinkman model; Maxwell model; Darcy model; differential transformation method	When cone is tilted→↑heat transfer; when cone is tilted→heat transfer being max	$0\% \le \phi \le 5\%$ $3.32 \times 10^5 \le Ra \le 6.7$ $\times 10^7$ $\epsilon = 0.99$
(Shah et al., 2023)	Heated stretching surface	TiO ₂ -engine oil	Darcy–Forchheimer model; thermal radiation; entropy generation	↑δ _e ,φ→↓heat profile; ↑Q, Rd, Ec→↓heat profile	$0.05 \le \varphi \le 0.4$ $0.1 \le \varepsilon \le 1.3$ $1 \le Q \le 1.8$ $0.1 \le Rd \le 1$ $1 \le Ec \le 1.9$
(Malik et al., 2023)	Rotating disk	Ag-TiO ₂	Modified Buongiorno model; MHD; thermal radition	↑Rd, Nt, Nb→↑temp profile; C_{F} →↑magnetic, Darcy- Forchheimer, velocity slip and ↓ δ ; ↑Nu→↑Nt, Nb	$0 \le \delta \le 1$ $0 \le Rd \le 3$ $0.4 \le Nb \le 1.6$ $0.3 \le Fr \le 5$ Sc = 1 Pr = 6.2
(Yasir et al., 2023)	Stretching/ shrinking disk; nonuniform heat source/sink	MgO/Ag–water	Hamilton–Crosser model	Inclusion of hybrid nanofluid→↑heat transport rate; ↑system's energy→↑heat radiation	Pr = 6.2 $Rd = 1$

TABLE 4: (continued)

Ref.	Geometry description	Nanofluid	Methodology	Results	Decision variables
(Mahabaleshwar et al., 2023)	Porous stretching/ sinking sheet	Ternary nanoffuid	Ordinary differential equations; radiation	With velocity profile become linear→↑Da; ↑suction→↑fluid and dusty velocity profile; ↑strength of the particle interaction parameter→↑solution domain thickness	$0 \le Da^{-1} \le 10$ $Pr = 2$ $Nr = 0.1$
(Al-hanaya et al., 2024)	Truncated cone	Pseudo-plastic, dilatant/ Newtonian nanoffuids	Non-Darcy model; Ostwald-de Waele model	↑Temp profile ratio→↓convective transport, Nu, Sh; thermal radiation→↑õT, nanoparticles; Arrhenius activation energy→best to get ↑Nu _x	$0.1 \le Nr \le 1$ $0.1 \le Nb \le 0.7$ $0.2 \le Nu \le 0.49$ $0.2 \le 10$ $0.2 \le 10$
(Raza et al., 2024)	Two-dimensional rotating porous channel	Cu/Al ₂ O ₃ /TiO ₂ – water	MHD; Runge–Kutta method	↑Re→↑wear stress heat transfer rate, ↓ Nu	Pr = 6.2 Re = -5.5
(Feng and wang., 2024)	I	Fe ₃ O ₄ -water	MHD; Boltzman method; double-diffusive convection	↑Le→↓heat transfer, ↑mass transfer ↑e→↑heat and mass exchange	$1 \le Le \le 5$ $0.2 \le \epsilon \le 0.8$ $0 \le Ha \le 60$ $2.96 \le Nu_{av} \le 4.66$ $Da = 10^{-2}$ $Ra = 10^{5}$ $\Phi = 0.04$
(Li et al., 2024)	Porous rotating disk	Maxwell nanofluid	MHD; bioconvection	↑Temp profile→↑Nb, ↓ φ ; †skin friction, Sh→↑ ω , ε	$\begin{array}{c} 1 \le \Pr \le 4 \\ 0.5 \le Sc \le 4 \\ 0.1 \le Nb \le 2.1 \end{array}$
(Li and You, 2023)	Porous media	Al ₂ O ₃ /Cu- water (mass- based hybrid nanofluid)	Mass-based hybrid nanofluid model for Homann stagnation point	↑Mass of nanoparticles→↑ Nu _x , ↑skin friction coefficient	Pr = 6.2 12.06% ≤ Shear stress ≤ 52.48%
(Lin et al., 2024)	Flat-plate solar collector	Al ₂ O ₃ /Cu–water	Darcy–Brinkman– Forchheimer; single-phase mixed model	↑Da→↑heat transfer performance within the channel; ↑φ→↑heat transfer	$10^{-5} \le Da \le 10^{#2}$ $1\% \le \phi \le 3\%$ $234 \le Re \le 468$

IABLE 4: (continued)	inued)				
(Saeed et al., 2020)	Porous stretching cylinder	Al ₂ O ₃ /Cu–water	Darcy–Forchheimer; MHD	∱F→†flow resistance; ↓φ(η)↑→†Sc	$3 \le Pr \le 6$ $0.2 \le Sc \le 1.7$ $1.2 \le N_t \le 1.8$ $0.1 \le F \le 0.8$
(You and Cui, 2023)	(You and Cui, Porous media 2023)	Al ₂ O ₃ /Cu-water Homotoy (spherical hybrid method nanofluid)	Homotopy analysis method	$\uparrow Nu_x \rightarrow \phi; \uparrow skin \ friction$ $coefficient \rightarrow \uparrow \phi$	Pr = 6.2 13.68% \leq shear stress \leq 74.69% 0.5% \leq ϕ \leq 20%

TABLE 5: Impact of nanofluid concentration and size on Nu: statistical analysis and literature review

Ref.	Nu	Volume fraction and size
(Martin et al., 2021)	Nu improves 65% at max Ra	$2.35 \times 10^5 \le \text{Ra} \le 5.13 \times 10^7;$ $0\% \le \phi \le 5\%$
(Miles and Bessaïh, 2021)	For Ra = 10 ⁵ the best Nu for Ag—water reaches 9.5%	$0 \le \varphi \le 0.01;$ $10^{-4} \le Da \le 10^{-1}$ $0.2 \le \varepsilon \le 0.99$
(Mehryan et al., 2020)	at Ra = 10^6 and $\phi = 0.05$; Nu is 9.76	$0\% \le \phi \le 5\% \ 0.2 \le Stefan \ number \le \infty$
(Esfe et al., 2022)	Nu_{av} increase with increasing Ra	$10^{-3} \le Ra \le 10^6$; $0\% \le \varphi \le 3\%$
(Tan et al., 2023)	Nu drops by 50.48% with increasing Ha	$0 \le Ha \le 50; \ 0 \le \phi \le 20$
(Alilat et al., 2023)	Nu _{avg} enhancement varies between 20% to 70%	$0\% \le \varphi \le 3\%$; $3.32 \times 10^5 \le 6.7 \times 10^7$
(Soleymai et al., 2022)	Nu increase 21% by adding nanoparticles	$0.2 \le \varepsilon \le 0.8;$ $0 \le \phi \le 0.025$
(Wang et al., 2021)	Nu increase 54.83% for Re = 13,000 in triangular tube	$0 \le Nu \le 300;$ $6000 \le \text{Re} \le 36000$
(Sivasankaran et al., 2022)	Nu increases from 150 to 450 (in Re = 4000 to 13,000)	$0.1 \le Gr \le 0.3;$ $0\% \le Q_{av} \le 5\%$
(Yeasmin et al., 2022)	Nu_{avg} for Da = 0.0001 is from 1.25 to 7.0	$0 \le \phi \le 0.01;$ $0.05 \le \epsilon \le 0.8$

6.6 Statistical Results

This section provides a statistical analysis of parameters reported in studies concerning nanofluids within porous media. A comprehensive literature review indicates that aluminum oxide nanoparticles suspended in water constitute the most frequently investigated nanofluid, comprising 28.33% of the analyzed research. Copper and iron oxide nanofluids in water follow as the second and third most common nanofluid types, representing 25% and 8.33% of the studies, respectively. A detailed breakdown of nanofluid share in the literature is presented in Table 6.

Alumina nanoparticles are widely employed due to their superior dispersion capabilities within base fluids. However, the stability of nanofluids within porous media is a paramount consideration. Metal oxide nanoparticles exhibit inconsistent influences on free convection heat transfer, with enhancements observed in some studies and reductions in others. Conversely, nanoparticles of all types generally augment heat transfer in forced convection environments. Cylindrical geometries were the most prevalent configuration studied, accounting for 27.78% of the research, fol-

TABLE 6: The share of each nanoparticle in published studies

Nanoparticle	Share (%)
Al ₂ O ₃ –water	28.33
Cu-water	25
Fe ₃ O ₄ –water	8.33
TiO ₂ -water	10
Ag-Mgo	5
Other	23.34

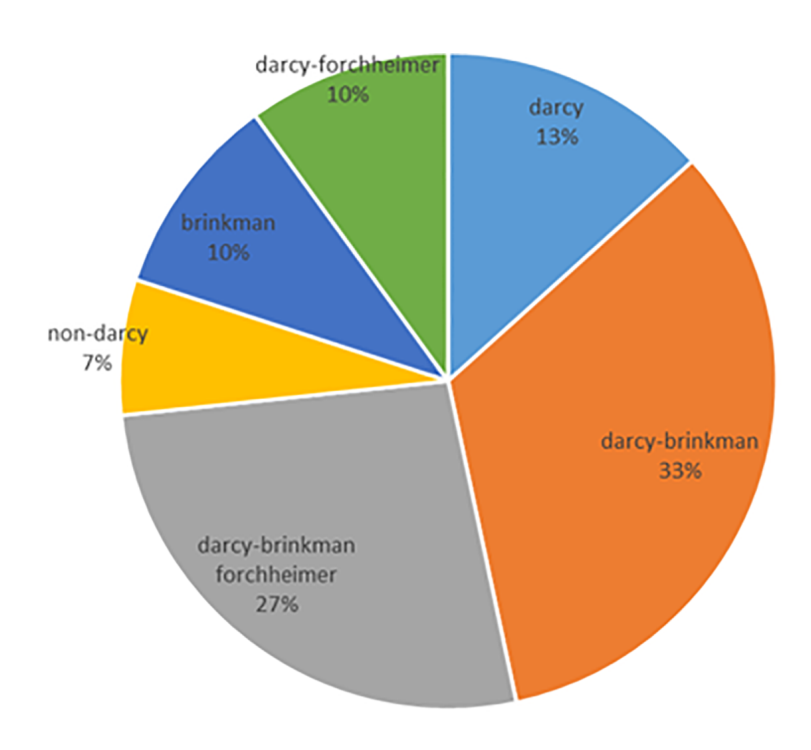
lowed by hole and circular geometries at 14.81% and 7.41%, respectively. A detailed overview of these findings is presented in Table 7.

Figure 6 presents a comparative analysis of models used in the reviewed studies. The Darcy–Brinkman model is the most frequently employed, accounting for 33% of the research. The Darcy–Brinkman–Forchheimer model follows with a 27% share, whereas the Darcy model represents 13% of the studies. These findings underscore the dominance of the Darcy–Brinkman and Darcy–Brinkman–Forchheimer models within the field of research.

Tables 1 through 4 suggest that MHD models constitute 39% of the models employed in studies involving magnetic fields. Figure 7 provides a breakdown of the contributions of major scientific publishers (i.e., Science Direct, Springer, MDPI, John Wiley, and ASME) to the research domain. Science Direct emerges as the predominant publishing platform, contributing 76% of the analyzed publications.

TABLE	/: The	share of	each	of the	studied	geometries	in publish	ed papers

Geometry	Share %
Square	7/4
Hole	14/81
Circular	7/41
Cylindrical	27/78
Cone	5/56
Other shapes	37/04



a darcy darcy-brinkman a darcy-brinkman forchheimer non-darcy brinkman darcy-forchheimer

FIG. 6: The share of the models used in the presence and absence of a magnetic field

The statistical analysis focused on parameters identified by authors as critical to heat transfer: nanoparticle type and geometric configuration. Given the prevalence of numerical modeling in the reviewed literature, the employed porous media flow models were also examined. Although not directly related to heat transfer, the impact of external forces, such as magnetic fields, on heat transfer is well established. Consequently, the inclusion of MHD models, comprising approximately 39% of the studies, was considered relevant to the overall analysis.

7. CONCLUSION

This study reviewed the literature published since 2020 on nanofluid heat transfer in porous media. Expanding on a previous review (Nabwey et al., 2023), this research employed a novel statistical approach to analyze recent articles. Results indicated that adding nanoparticles to the base fluid enhances heat transfer. However, increasing the nanoparticle volume fraction intensifies the viscosity effect, which can hinder heat transfer despite improved thermal conductivity. Moreover, an increased nanoscale conductivity relative to the porous matrix leads to decreased heat transfer. Conversely, heat transfer improves with increasing Da and porosity. These findings highlight the complex interplay between nanoparticle concentration, viscosity, and porous medium properties in determining heat transfer performance. The most significant findings of this study are as follows:

- The highest heat transfer coefficient and Nu for the nanoparticles were observed at a 30° angle with a square porosity, whereas the lowest values were recorded at a 0° angle.
- In forced convection, heat transfer was enhanced with increasing Ha and porosity. For instance, in a tube with a porous hemisphere, increased porosity (up to 0.8) and Ha increased the Nu.
- For hybrid nanofluids in a porous medium filled with TiO₂-Ag—water, increasing the length of the heat source
 and the number of waves improved the average heat transfer, as indicated by the average Nu. Conversely,
 increasing the Ha reduced the average Nu.

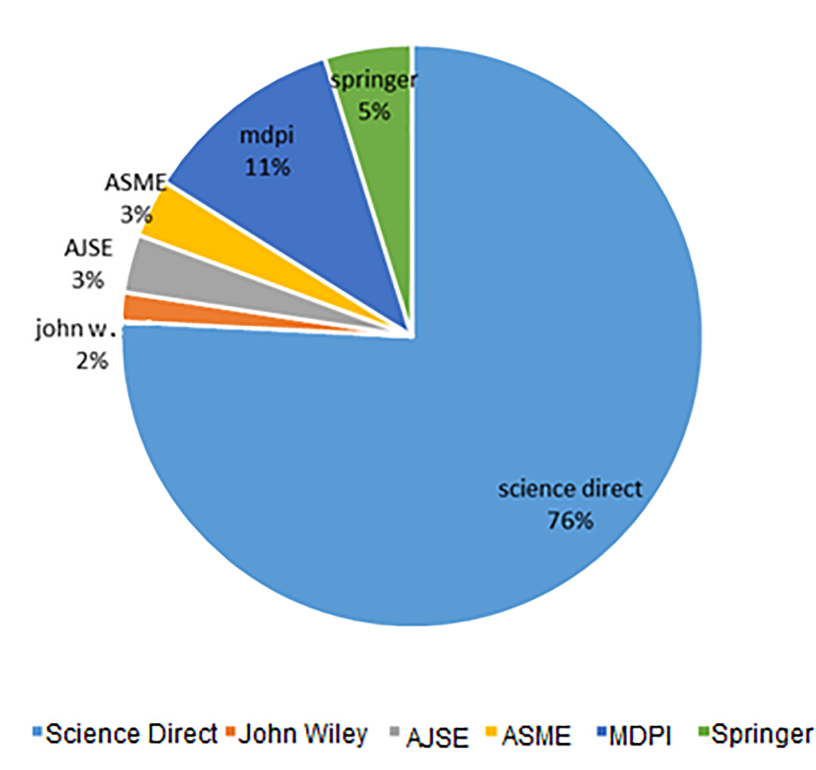


FIG. 7: The contribution of each publisher of the published papers related to nanofluids in a porous material

The results indicate that parameters such as the type and volume fraction of nanoparticles, the geometry of the porous medium, and the application of magnetic fields significantly enhance heat transfer.

ACKNOWLEDGMENT

The authors extend their appreciation to Prince Sattam bin Abdulaziz University for funding this research work through the Project No. (2024/RV/14).

AUTHOR CONTRIBUTIONS

All authors contributed equally to this work. All authors have read and agreed to the published version of the manuscript.

REFERENCES

- Abbas, W., Ibrahim, M.A., Mokhtar, O., Megahed, A.M., and Said, A.A., Numerical Analysis of MHD Nanofluid Flow Characteristics with Heat and Mass Transfer over a Vertical Cone Subjected to Thermal Radiations and Chemical Reaction, *J. Nonlinear Math. Phys.*, vol. **2023**, pp. 1–27, 2023.
- Abderrahmane, A.I.S.S.A., Hatami, M., Medebber, M.A., Haroun, S., Ahmed, S.E., and Mohammed, S., Non-Newtonian Nanofluid Natural Convective Heat Transfer in an Inclined Half-Annulus Porous Enclosure Using FEM, *Alex. Eng. J.*, vol. **61**, no. 7, pp. 5441–5453, 2022.
- Abderrahmane, A., Jamshed, W., Abed, A.M., Smaisim, G.F., Guedri, K., Akbari, O.A., and Baghaei, S., Heat and Mass Transfer Analysis of Non-Newtonian Power-Law Nanofluid Confined within Annulus Enclosure Using Darcy-Brinkman-Forchheimer Model, *Case Stud. Therm. Eng.*, vol. 40, p. 102569, 2022.
- Agrawal, P., Dadheech, P.K., Jat, R.N., Nisar, K.S., Bohra, M., and Purohit, S.D., Magneto Marangoni Flow of γ-Al₂O₃ Nanofluids with Thermal Radiation and Heat Source/Sink Effects over a Stretching Surface Embedded in Porous Medium, *Case Stud. Therm. Eng.*, vol. **23**, p. 100802, 2021.
- Al Qarni, A.A., Elsaid, E.M., Abdel-Aty, A.H., and Eid, M.R., Heat Transfer Efficacy and Flow Progress of Tripartite Diffusion in Magneto-Radiative Reiner-Philippoff Nanofluid in Porous Darcy–Forchheimer Substance with Heat Source, *Case Stud. Therm. Eng.*, vol. **45**, p. 103022, 2023.
- Al-Amir, Q.R., Hamzah, H.K., Ali, F.H., Hatami, M., Al-Kouz, W., Al-Manea, A., and Alahmer, A., Investigation of Natural Convection and Entropy Generation in a Porous Titled Z-Staggered Cavity Saturated by TiO₂–Water Nanofluid, *Int. J. Thermofluids*, vol. 19, p. 100395, 2023.
- Alghamdi, M., Wakif, A., Thumma, T., Khan, U., Baleanu, D., and Rasool, G., Significance of Variability in Magnetic Field Strength and Heat Source on the Radiative-Convective Motion of Sodium Alginate-Based Nanofluid within a Darcy-Brinkman Porous Structure Bounded Vertically by an Irregular Slender Surface, *Case Stud. Therm. Eng.*, vol. 28, p. 101428, 2021.
- Al-hanaya, A., Rashed, Z.Z., and Ahmed, S.E., Radiative Flow of Temperature-Dependent Viscosity Power-Law Nanofluids over a Truncated Cone Saturated Heat Generating, Porous Media: Impacts of Arrhenius Energy, *Case Stud. Therm. Eng.*, vol. **53**, p. 103874, 2024.
- Alilat, N., Sastre, F., Martín-Garín, A., Velazquez, A., and Baïri, A., Heat Transfer in a Conical Gap Using H₂O-Cu Nanofluid and Porous Media. Effects of the Main Physical Parameters, *Case Stud. Therm. Eng.*, vol. 47, p. 103026, 2023.
- Alsedais, N., Aly, A.M., and Mansour, M.A., Local Thermal Non-Equilibrium Condition on Mixed Convection of a Nanofluid-Filled Undulating Cavity Containing Obstacle and Saturated by Porous Media, *Ain Shams Eng. J.*, vol. 13, no. 2, p. 101562, 2022.
- Amine, B.M., Redouane, F., Mourad, L., Jamshed, W., Eid, M.R., and Al-Kouz, W., Magnetohydrodynamics Natural Convection of a Triangular Cavity Involving Ag-MgO/Water Hybrid Nanofluid and Provided with Rotating Circular Barrier and a Quarter Circular Porous Medium at Its Right-Angled Corner, *Arab. J. Sci. Eng.*, vol. **46**, no. 12, pp. 12573–12597, 2021.
- Aminian, E., Moghadasi, H., Saffari, H., and Gheitaghy, A.M., Investigation of Forced Convection Enhancement and Entropy Generation of Nanofluid Flow through a Corrugated Minichannel Filled with a Porous Media, *Entropy*, vol. **22**, no. 9, p. 1008, 2020
- Arafa, A.A., Ahmed, S.E., and Allan, M.M., Peristaltic Flow of Non-Homogeneous Nanofluids through Variable Porosity and Heat Generating Porous Media with Viscous Dissipation: Entropy Analyses, *Case Stud. Therm. Eng.*, vol. **32**, p. 101882, 2022.

Armaghani, T., Rashad, A.M., Togun, H., Mansour, M.A., and Salah, T., Hybrid Nanofluid Unsteady MHD Natural Convection in an Inclined Wavy Porous Enclosure with Radiation Effect, Partial Heater and Heat Generation/Absorption, *Iran. J. Sci. Technol. Trans. Mech. Eng.*, pp. 1–18, 2024.

- Azizimehr, B., Armaghani, T., Ghasemiasl, R., Nejadian, A.K., and Javadi, M.A., A Comprehensive Review of Recent Developments in Hydrogen Production Methods Using a New Parameter, *Int. J. Hydrogen Energy*, vol. **72**, pp. 716–729, 2024.
- Bairi, A., Porous Materials Saturated with Water-Copper Nanofluid for Heat Transfer Improvement between Vertical Concentric Cones, *Int. Commun. Heat Mass Transf.*, vol. **126**, p. 105439, 2021.
- Bakar, S.A., Arifin, N.M., Bachok, N., and Ali, F.M., Effect of Thermal Radiation and MHD on Hybrid Ag-TiO₂/H₂O Nanofluid past a Permeable Porous Medium with Heat Generation, *Case Stud. Therm. Eng.*, vol. **28**, p. 101681, 2021.
- Choi, S.U. and Eastman, J.A., Enhancing Thermal Conductivity of Fluids with Nanoparticles, Argonne National Lab., Argonne, IL. 1995.
- Esfe, M.H., Rostamian, H., Toghraie, D., Hekmatifar, M., and Abad, A.T.K., Numerical Study of Heat Transfer of U-Shaped Enclosure Containing Nanofluids in a Porous Medium Using Two-Phase Mixture Method, *Case Stud. Therm. Eng.*, vol. 38, p. 102150, 2022.
- Farahani, S.D. and Alizadeh, A.A., Thermal Efficiency of Microchannel Heat Sink: Incorporating Nano-Enhanced Phase Change Materials and Porous Foam Gradient and Artificial Intelligence-Based Prediction, *Alex. Eng. J.*, vol. **82**, pp. 1–15, 2023.
- Farahani, S.D., Amiri, M., Majd, B.K., and Mosavi, A., Effect of Magnetic Field on Heat Transfer from a Channel: Nanofluid Flow and Porous Layer Arrangement, Case Stud. Therm. Eng., vol. 28, p. 101675, 2021.
- Feng, Y. and Wang, C., Lattice Boltzmann Study on Magnetohydrodynamic Double-Diffusive Convection in Fe₃O₄–H₂O Nanofluid-Filled Porous Media, *Case Stud. Therm. Eng.*, p. 104405, 2024.
- Flickinger, M.C., Ed., *Downstream Industrial Biotechnology: Recovery and Purification*, Hoboken, NJ: John Wiley & Sons, 2013. Ghali, D., Redouane, F., Abdelhak, R., Belhadj Mahammed, A., Zineb, C.D., Jamshed, W., and Mohd Nasir, N.A.A., Mathematical Entropy Analysis of Natural Convection of MWCNT—Fe₃O₄/Water Hybrid Nanofluid with Parallel Magnetic Field via Galerkin Finite Element Process, *Symmetry*, vol. 14, no. 11, p. 2312, 2022.
- Ghasemiasl, R., Hashemi, S., Armaghani, T., Tayebi, T., and Pour, M.S., Recent Studies on the Forced Convection of Nano-Fluids in Channels and Tubes: A Comprehensive Review, *Exp. Tech.*, vol. 47, no. 1, pp. 47–81, 2023.
- Girish, R., Salma, A., Subray, P.A., Hanumagowda, B.N., Varma, S.V.K., Nagaraja, K.V., and and Gamaoun, F., Effect of Temperature-Dependent Internal Heat Generation over Exponential and Dovetail Convective-Radiative Porous Fin Wetted in Hybrid Nanofluid, *Case Stud. Therm. Eng.*, vol. **49**, p. 103214, 2023.
- Habibishandiz, M. and Saghir, Z., MHD Mixed Convection Heat Transfer of Nanofluid Containing Oxytactic Microorganisms inside a Vertical Annular Porous Cylinder, *Int. J. Thermofluids*, vol. **14**, p. 100151, 2022.
- Habibishandiz, M., Saghir, Z., and Zahmatkesh, I., Thermo-Bioconvection Performance of Nanofluid Containing Oxytactic Microorganisms inside a Square Porous Cavity under Constant and Periodic Temperature Boundary Conditions, *Int. J. Thermofluids*, vol. 17, p. 100269, 2023.
- Hashemi, S., Armaghani, T., and Ghasemiasl, R., 3D Numerical Study of Al₂O₃—Water Nanofluid Unsteady Natural Convection via Using Oscillating Plate by Two-Way FSI Analysis, *J. Therm. Anal. Calorim.*, pp. 1–16, 2024.
- Hasnain, J., Abid, N., Alansari, M.O., and Ullah, M.Z., Analysis on Cattaneo-Christov Heat Flux in Three-Phase Oscillatory Flow of Non-Newtonian Fluid through Porous Zone Bounded by Hybrid Nanofluids, *Case Stud. Therm. Eng.*, vol. **35**, p. 102074, 2022.
- Holman, J.P., Heat Transfer, 9th ed., New York: McGraw-Hill, 1997.
- Hosseinzadeh, K., Moghaddam, M.E., Nateghi, S., Shafii, M.B., and Ganji, D.D., Radiation and Convection Heat Transfer Optimization with MHD Analysis of a Hybrid Nanofluid within a Wavy Porous Enclosure, *J. Magn. Magn. Mater.*, vol. **566**, p. 170328, 2023.
- Hussain, M. and Sheremet, M., Convective-Radiative Magnetized Dissipative Nanofluid (CNTs-Water) Transport in Porous Media, Using Darcy-Brinkman-Forchheimer Model, *Int. Commun. Heat Mass Transf.*, vol. **139**, p. 106420, 2022.
- Hussain, S., Pour, M.S., Jamal, M., and Armaghani, T., MHD Mixed Convection and Entropy Analysis of Non-Newtonian Hybrid Nanofluid in a Novel Wavy Elbow-Shaped Cavity with a Quarter Circle Hot Block and a Rotating Cylinder, *Exp. Tech.*, vol. 47, no. 1, pp. 17–36, 2023.
- Hussain, S., Tayebi, T., Armaghani, T., Rashad, A.M., and Nabwey, H.A., Conjugate Natural Convection of Non-Newtonian Hybrid Nanofluid in Wavy-Shaped Enclosure, *Appl. Math. Mech.*, vol. **43**, no. 3, pp. 447–466, 2022.
- Jakeer, S., Reddy, P.B., Rashad, A.M., and Nabwey, H.A., Impact of Heated Obstacle Position on Magneto-Hybrid Nanofluid Flow in a Lid-Driven Porous Cavity with Cattaneo-Christov Heat Flux Pattern, *Alex. Eng. J.*, vol. **60**, no. 1, pp. 821–835, 2021.
- Jegadheeswaran, S. and and Pohekar, S.D., Performance Enhancement in Latent Heat Thermal Storage System: A Review, *Renew. Sustain. Energy Rev.*, vol. 13, no. 9, pp. 2225–2244, 2009.

- Jiang, X., Hatami, M., Abderrahmane, A., Younis, O., Makhdoum, B.M., and Guedri, K., Mixed Convection Heat Transfer and Entropy Generation of MHD Hybrid Nanofluid in a Cubic Porous Cavity with Wavy Wall and Rotating Cylinders, *Appl. Therm. Eng.*, vol. 226, p. 120302, 2023.
- Kaviany, M., Principles of Heat Transfer in Porous Media, Berlin: Springer Science and Business Media, 2012.
- Khalili, R., Tavousi, E., Kazerooni, R.B., Noghrehabadi, A., and Taheripour, S., Lattice Boltzmann Method Simulation of Nanofluid Natural Convection Heat Transfer in a Square Cavity with Constant Heat Flux at Walls, *Iran. J. Sci. Technol. Trans. Mech. Eng.*, vol. **2024**, pp. 1–16, 2024.
- Khan, U., Zaib, A., Ishak, A., Sherif, E.S.M., Waini, I., Chu, Y.M., and Pop, I., Radiative Mixed Convective Flow Induced by Hybrid Nanofluid over a Porous Vertical Cylinder in a Porous Media with Irregular Heat Sink/Source, *Case Stud. Therm. Eng.*, vol. **30**, p. 101711, 2022.
- Kodi, R., Ganteda, C., Dasore, A., Kumar, M. L., Laxmaiah, G., Hasan, M.A., and Razak, A., Influence of MHD Mixed Convection Flow for Maxwell Nanofluid through a Vertical Cone with Porous Material in the Existence of Variable Heat Conductivity and Diffusion, *Case Stud. Therm. Eng.*, vol. **44**, p. 102875, 2023.
- Li, S., Faizan, M., Ali, F., Ramasekhar, G., Muhammad, T., Khalifa, H.A.E.W., and Ahmad, Z., Modelling and Analysis of Heat Transfer in MHD Stagnation Point Flow of Maxwell Nanofluid over a Porous Rotating Disk, *Alex. Eng. J.*, vol. **91**, pp. 237–248, 2024.
- Li, S. and You, X., Shape-Factor Impact on a Mass-Based Hybrid Nanofluid Model for Homann Stagnation-Point Flow in Porous Media, *Nanomaterials*, vol. **13**, no. 6, p. 984, 2023.
- Li, Y.X., Alshbool, M.H., Lv, Y.P., Khan, I., Khan, M.R., and Issakhov, A., Heat and Mass Transfer in MHD Williamson Nanofluid Flow over an Exponentially Porous Stretching Surface, *Case Stud. Therm. Eng.*, vol. **26**, p. 100975, 2021.
- Lin, X., Xia, Y., Cheng, Z., Liu, X., Fu, Y., Li, L., and Zhou, W., Thermal Performance Analysis of Porous Foam-Assisted Flat-Plate Solar Collectors with Nanofluids, *Sustainability*, vol. **16**, no. 2, p. 693, 2024.
- Liu, H., Li, C., and Sun, J., Magnetohydrodynamic Influence on Fractional Nanofluid Convection in Infinite Vertical Porous Media with Constant Heat Flux, *Alex. Eng. J.*, vol. **95**, pp. 224–235, 2024.
- Mahabaleshwar, U.S., Maranna, T., Perez, L.M., Bognar, G.V., and Oztop, H.F., An Impact of Radiation on Laminar Flow of Dusty Ternary Nanofluid over Porous Stretching/Shrinking Sheet with Mass Transpiration, *Results Eng.*, vol. 18, p. 101227, 2023.
- Malik, M.F., Shah, S.A.A., Bilal, M., Hussien, M., Mahmood, I., Akgul, A., and Az-Zo'bi, E.A., New Insights into the Dynamics of Heat and Mass Transfer in a Hybrid (Ag-TiO₂) Nanofluid Using Modified Buongiorno Model: A Case of a Rotating Disk, *Results Phys.*, vol. **53**, p. 106906, 2023.
- Mandal, D.K., Mondal, M.K., Biswas, N., Manna, N.K., Al-Farhany, K., Mitra, A., and Chamkha, A.J., Convective Heat Transport in a Porous Wavy Enclosure: Nonuniform Multi-Frequency Heating with Hybrid Nanofluid and Magnetic Field, *Heliyon*, vol. **2024**, 2024.
- Maneengam, A., Bouzennada, T., Abderrahmane, A., Ghachem, K., Kolsi, L., Younis, O., and Weera, W., Numerical Study of 3D MHD Mixed Convection and Entropy Generation in Trapezoidal Porous Enclosure Filled with a Hybrid Nanofluid: Effect of Zigzag Wall and Spinning Inner Cylinder, *Nanomaterials*, vol. 12, no. 12, p. 1974, 2022.
- Mansour, M.A., Rashad, A.M., Togun, H., Salah, T., and Armaghani, T., Unsteady MHD Hybrid Nanofluid Mixed Convection Heat Transfer in a Wavy Porous Cavity with Thermal Radiation, *J. Therm. Anal. Calorim.*, vol. **149**, no. 5, pp. 2425–2442, 2024.
- Martin, E., Sastre, F., Velazquez, A., and Baïri, A., Heat Transfer Enhancement around a Finned Vertical Antenna by Means of Porous Media Saturated with Water-Copper Nanofluid, *Case Stud. Therm. Eng.*, vol. **28**, p. 101555, 2021.
- Meghdadi Isfahani, A.H., Parametric Study of Rarefaction Effects on Micro- and Nanoscale Thermal Flows in Porous Structures, *J. Heat Transf.*, vol. **139**, no. 9, p. 092601, 2017.
- Mehling, H. and Cabeza, L.F., Heat and Cold Storage with PCM, Heat Mass Transf., pp. 11-55, 2008.
- Mehryan, S.A.M., Ismael, M., and Ghalambaz, M., Local Thermal Nonequilibrium Conjugate Natural Convection of Nano-Encapsulated Phase Change Particles in a Partially Porous Enclosure, *Math. Methods Appl. Sci.*, vol. **2020**, 2020.
- Memon, M.A., Khan, M.S., Saleem, S., Eldin, S.M., and Jacob, K., Heat Transfer through a Higher Grade Forchheimer Porous CuO-H₂O-Nano-Medium Confined between Non-Isothermal Moving Plates, *Case Stud. Therm. Eng.*, vol. 47, p. 103035, 2023
- Miles, A. and Bessaïh, R., Heat Transfer and Entropy Generation Analysis of Three-Dimensional Nanofluids Flow in a Cylindrical Annulus Filled with Porous Media, *Int. Commun. Heat Mass Transf.*, vol. **124**, p. 105240, 2021.
- Moltames, R., Azizimehr, B., and Assareh, E., Energy and Exergy Efficiency Improvement of a Solar Driven Trigeneration System Using Particle Swarm Optimization Algorithm, *J. Sol. Energy Res.*, vol. 4, no. 1, pp. 31–39, 2019.
- Nabwey, H.A., Armaghani, T., Azizimehr, B., Rashad, A.M., and Chamkha, A.J., A Comprehensive Review of Nanofluid Heat Transfer in Porous Media, *Nanomaterials*, vol. **13**, no. 5, p. 937, 2023.

Nazarahari, M., Ghasemi Asl, R., and Armaghani, T., Experimental Study of Nanofluids Natural Convection Heat Transfer in Various Shape Pores of Porous Media, J. Therm. Anal. Calorim., vol. 149, no. 5, pp. 2331–2349, 2024.

- Nazari, M., Kayhani, M.H., and Bagheri, A.A.H., Comparison of Heat Transfer in a Cavity between Vertical and Horizontal Porous Layers Using LBM, *Modares Mech. Eng.*, vol. 13, no. 8, pp. 93–107, 2013.
- Nemati, M., Farahani, S.D., and Armaghani, T., A LBM Entropy Calculation Caused by Hybrid Nanofluid Mixed Convection under the Effect of Changing the Kind of Magnetic Field and Other Active/Passive Methods, *J. Magn. Magn. Mater.*, vol. **566**, p. 170277, 2023.
- Rana, P., Mahanthesh, B., Nisar, K.S., Swain, K., and Devi, M., Boundary Layer Flow of Magneto-Nanomicropolar Liquid over an Exponentially Elongated Porous Plate with Joule Heating and Viscous Heating: A Numerical Study, *Arab. J. Sci. Eng.*, vol. 46, no. 12, pp. 12405–12415, 2021.
- Rashad, A.M., Armaghani, T., Sadeghi, M.S., Mansour, M.A., Chamkha, A.J., Dogonchi, A.S., and Nabwey, H.A., MHD Mixed Convection of Localized Heat Source/Sink in an Al₂O₃-Cu/Water Hybrid Nanofluid in L-Shaped Cavity, *Alex. Eng. J.*, vol. 60, no. 3, pp. 2947–2962, 2021.
- Rashed, Z.Z., Alhazmi, M., and Ahmed, S.E., Non-Homogenous Nanofluid Model for 3D Convective Flow in Enclosures Filled with Hydrodynamically and Thermally Heterogeneous Porous Media, *Alex. Eng. J.*, vol. **60**, no. 3, pp. 3119–3132, 2021.
- Raza, Q., Wang, X., Muhammed, H.A., Ali, B., Ali, M.R., and Hendy, A.S., Numerically Analyzed of Ternary Hybrid Nanofluids Flow of Heat and Mass Transfer Subject to Various Shapes and Size Factors in Two-Dimensional Rotating Porous Channel, Case Stud. Therm. Eng., vol. 56, p. 104235, 2024.
- Reddy, N.K., Swamy, H.K., Sankar, M., and Jang, B., MHD Convective Flow of Ag-TiO₂ Hybrid Nanofluid in an Inclined Porous Annulus with Internal Heat Generation, *Case Stud. Therm. Eng.*, vol. **42**, p. 102719, 2023.
- Sadighi, S., Jabbari, M., Afshar, H., and Ashtiani, H.A.D., MHD Heat and Mass Transfer Nanofluid Flow on a Porous Cylinder with Chemical Reaction and Viscous Dissipation Effects: Benchmark Solutions, *Case Stud. Therm. Eng.*, vol. 40, p. 102443, 2022.
- Saeed, A., Tassaddiq, A., Khan, A., Jawad, M., Deebani, W., Shah, Z., and Islam, S., Darcy-Forchheimer MHD Hybrid Nanofluid Flow and Heat Transfer Analysis over a Porous Stretching Cylinder, *Coatings*, vol. 10, no. 4, p. 391, 2020.
- Saghir, M.Z., Welsford, C., Thanapathy, P., Bayomy, A.M., and Delisle, C., Experimental Measurements and Numerical Computation of Nano Heat Transfer Enhancement inside a Porous Material, J. Therm. Sci. Eng. Appl., vol. 12, no. 1, p. 011003, 2020.
- Sajjadi, H., Mansouri, N., Nabavi, S.N., Delouei, A.A., and Atashafrooz, M., Sensitivity Analysis of Natural Convection in a Porous Cavity Filled with Nanofluid and Equipped with Horizontal Fins Using Various Optimization Methods and MRT-LB, *Sci. Rep.*, vol. **14**, no. 1, p. 9847, 2024.
- Salehi, M., Afshar, S.R., Ali, R., and Chamkha, A.J., Numerical Investigation of TiO₂—Water Nanofluid Heat Transfer in a Porous Wavy Circular Chamber with a —Shaped Heater under Magnetic Field, *Case Stud. Therm. Eng.*, vol. 49, p. 103405, 2023.
- Sedki, A.M., Effect of Thermal Radiation and Chemical Reaction on MHD Mixed Convective Heat and Mass Transfer in Nanofluid Flow Due to Nonlinear Stretching Surface through Porous Medium, *Results Mater.*, vol. 16, p. 100334, 2022.
- Shah, Z., Shafiq, A., Rooman, M., Alshehri, M.H., and Bonyah, E., Darcy–Forchhemier Prandtl–Eyring Nanofluid Flow with Variable Heat Transfer and Entropy Generation Using Cattaneo-Christov Heat Flux Model: Statistical Approach, *Case Stud. Therm. Eng.*, vol. **49**, p. 103376, 2023.
- Sivasankaran, S. and Bhuvaneswari, M., Numerical Study on Influence of Water Based Hybrid Nanofluid and Porous Media on Heat Transfer and Pressure Loss, *Case Stud. Therm. Eng.*, vol. **34**, p. 102022, 2022.
- Soleymani, P., Ma, Y., Saffarifard, E., Mohebbi, R., Babaie, M., Karimi, N., and Saedodin, S., Numerical Investigation on Turbulent Flow, Heat Transfer, and Entropy Generation of Water-Based Magnetic Nanofluid Flow in a Tube with Hemisphere Porous under a Uniform Magnetic Field, *Int. Commun. Heat Mass Transf.*, vol. 137, p. 106308, 2022.
- Sultana, U., Mushtaq, M., Muhammad, T., and Albakri, A., On Cattaneo-Christov Heat Flux in Carbon-Water Nanofluid Flow Due to Stretchable Rotating Disk through Porous Media, *Alex. Eng. J.*, vol. **61**, no. 5, pp. 3463–3474, 2022.
- Tan, X., Altoum, S.H., Othman, H.A., Syam, M.I., Salman, M.A., and Musa, A., Thermal Analysis of Nanofluid Flow within Porous Enclosure with Curved Hot Wall Utilizing Numerical Approach, *Case Stud. Therm. Eng.*, vol. **45**, p. 102923, 2023.
- Tayebi, T., Dahmane, F., Jamshed, W., Chamkha, A.J., El Din, S.M., and Raizah, Z., Double-Diffusive Magneto-Natural Convection of Nanofluid in an Enclosure Equipped with a Wavy Porous Cylinder in the Local Thermal Non-Equilibrium Situation, *Case Stud. Therm. Eng.*, vol. **43**, p. 102785, 2023.
- Udoh, I.I., Ekerenam, O.O., Daniel, E.F., Ikeuba, A.I., Njoku, D.I., Kolawole, S.K., and Uzoma, P.C., Developments in Anticorrosive Organic Coatings Modulated by Nano/Microcontainers with Porous Matrices, *Adv. Colloid Interface Sci.*, p. 103209, 2024.
- Wang, J., Xu, Y.P., Qahiti, R., Jafaryar, M., Alazwari, M.A., Abu-Hamdeh, N.H., and Selim, M.M., Simulation of Hybrid Nanofluid Flow within a Microchannel Heat Sink Considering Porous Media Analyzing CPU Stability, *J. Pet. Sci. Eng.*, vol. **208**, p. 109734, 2022.

- Wang, Y., Qi, C., Ding, Z., Tu, J., and Zhao, R., Numerical Simulation of Flow and Heat Transfer Characteristics of Nanofluids in Built-In Porous Twisted Tape Tube, *Powder Technol.*, vol. **392**, pp. 570–586, 2021.
- Yasir, M., Khan, M., Alqahtani, A.S., and Malik, M.Y., Numerical Study of Axisymmetric Hybrid Nanofluid MgO-Ag/H₂O Flow with Non-Uniform Heat Source/Sink, *Alex. Eng. J.*, vol. **75**, 439–446, 2023.
- Yeasmin, S., Billah, M.M., Molla, M.Z., and Hoque, K.E., Numerical Analysis of Unsteady Mixed Convection Heat Transfer Characteristics of Nanofluids Confined within a Porous Lid-Driven L-Shaped Cavity, *Int. J. Thermofluids*, vol. 16, p. 100218, 2022.
- You, X. and Cui, J., Spherical Hybrid Nanoparticles for Homann Stagnation-Point Flow in Porous Media via Homotopy Analysis Method, *Nanomaterials*, vol. **13**, no. 6, p. 1000, 2023.